IMPROVING DIFFERENTIAL DETECTION OF MDPSK BY NOISE PREDICTION

Robert Schober, Wolfgang H. Gerstacker, and Johannes B. Huber

Lehrstuhl für Nachrichtentechnik II
Universität Erlangen-Nürnberg
Cauerstraße 7/NT, D-91058 Erlangen, Germany
e-mail: schober@nt.e-technik.uni-erlangen.de

ABSTRACT

A new technique is proposed to improve the performance of differential detection of MDPSK (M–ary differential phase–shift keying) significantly by reducing the noise in the decision variable by means of noise prediction. A nonlinear time–variant FIR or IIR structure is used for the prediction–error filter. For both filter structures the optimum filter coefficients are derived, assuming transmission over an additive white Gaussian noise (AWGN) channel. For the IIR structure a setting for the filter coefficient exists which yields a high performance for both AWGN and flat fading (Rayleigh and Ricean) channels. Moreover, a simple decision rule is derived for the IIR structure which allows an implementation with very low computational complexity.

1. INTRODUCTION

It is well known, that differential detection (DD) of MDPSK (M–ary differential phase–shift keying) is very attractive when simplicity and robustness of implementation are more important than achieving optimum power efficiency. In addition, tracking of the correct carrier phase, as required by coherent detection (CD), may be difficult or even impossible in a fading environment. On the other hand, in an additive white Gaussian noise (AWGN) environment, DD causes a performance loss compared to CD. This penalty becomes significant especially for $M \geq 4$. For example, at a bit error rate (BER) of 10^{-5} there is a penalty of 2.2 dB and 2.5 dB in power efficiency for $M = 4$ and $M = 8$, respectively. In literature, modified noncoherent detection schemes with an improved performance for AWGN channels have been proposed. For example, a maximum–likelihood receiver using multiple–symbol detection (MSD) was reported by Divsalar et al. [1]. The main disadvantage of MSD is its high computational complexity. Even a proposed fast algorithm [2] for MSD is very complex compared to techniques, which rely on feeding back previously decided symbols [3, 4, 5, 7, 8]. Especially the structure presented in [4] and [5] (in both papers the same filter structure was used as has been pointed out in [6]) is very attractive for implementation because it uses a simple one tap IIR filter to stabilize the reference phase before DD is performed. Hence, the new detector proposed here will be compared with this structure.

Phase detection techniques discarding any amplitude information as described in [7, 8] are not considered in the following since simulation results in [7] indicate that they degrade severely under fading conditions.

Although the detector presented here uses decision feedback, too, our approach is different from the previous ones. After conversion to complex baseband representation and sampling, the current received symbol is multiplied by the previous conjugated one, like in a conventional differential detector. Then a detection with embedded noise prediction follows. The scheme has a very low computational complexity and performs significantly better than conventional DD. For example, for an AWGN channel and $M = 4$ the improvement is about 1.2 dB at a BER of 10^{-3}. Moreover, our detector is more robust under flat Rayleigh and Ricean fading conditions than other low complexity decision feedback schemes [4, 5] as will be shown by simulations.

2. TRANSMISSION MODEL

Fig. 1 shows a block diagram of the transmission model under consideration. All signals are represented by

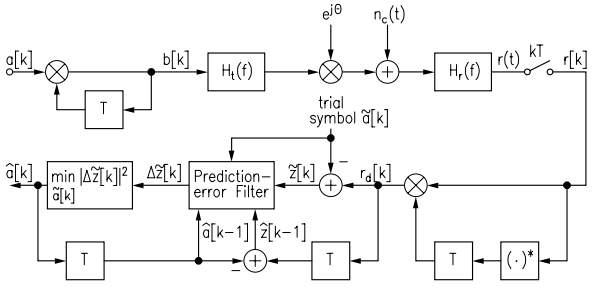

Figure 1: Block diagram of the transmission model for AWGN channel and constant phase shift Θ.

their complex–valued baseband equivalents. The MDPSK symbols are denoted by $a[k] \in \mathcal{A} = \{e^{j2\pi\frac{\nu}{M}} | \nu \in$

$\{0, 1, \ldots, M-1\}\}$ and the corresponding differentially encoded symbols $b[k]$ are given by

$$b[k] = a[k]b[k-1]. \tag{1}$$

Transmitter filter $H_t(f)$ and receiver filter $H_r(f)$ have square–root Nyquist characteristic. Hence, no intersymbol interference occurs as long as the signals are transmitted over AWGN or slow flat small–scale fading [9] channels. For the derivation of the noise prediction–error filters an AWGN channel with an arbitrary, constant phase shift Θ is assumed. In Section 5, the performance of the new receiver is also tested for flat Rayleigh and Ricean fading channels. The complex–valued additive white Gaussian noise with double–sided power spectral density N_0 (i.e., the single–sided power spectral density of the real passband noise is N_0, too, as usual) is denoted by $n_c(t)$. The samples $r[k]$ of the received signal $r(t)$ can be written as

$$r[k] = r(kT) = \mathrm{e}^{j\Theta} b[k] + n_0[k], \tag{2}$$

applying an appropriate normalization to $H_r(f)$. Here, T is the symbol interval and $n_0[k]$ denotes uncorrelated Gaussian noise with variance $\sigma^2 = \frac{N_0}{E_S}$, where E_S is the received energy per symbol.

Like in a conventional differential detector, the current received symbol $r[k]$ is multiplied by the previous conjugated one:

$$r_d[k] = r[k]r^*[k-1], \tag{3}$$

where $(\cdot)^*$ denotes complex conjugation. A conventional differential detector directly uses $r_d[k]$ to decide upon $a[k]$. The new receiver, however, first reduces the noise in the decision variable and therefore provides a better performance. Using Eqs. (1) and (2), Eq. (3) can be rewritten according to

$$\begin{aligned} r_d[k] = a[k] &+ \mathrm{e}^{j\Theta} b[k] n_0^*[k-1] + \mathrm{e}^{-j\Theta} b^*[k-1] n_0[k] \\ &+ n_0[k] n_0^*[k-1], \end{aligned} \tag{4}$$

and by introducing $n[k] \triangleq \mathrm{e}^{-j\Theta} n_0[k]$,

$$r_d[k] = a[k] + b[k]n^*[k-1] + b^*[k-1]n[k] + n[k]n^*[k-1] \tag{5}$$

is obtained. Note, that $n[k]$ is still uncorrelated Gaussian noise with the same variance as $n_0[k]$. By subtracting $a[k]$ from $r_d[k]$ the effective noise $z[k]$ can be calculated. However, since $a[k]$ is unknown at the receiver, a trial symbol $\tilde{a}[k] \in \mathcal{A}$, which takes on all M possible values of $a[k]$, is subtracted and $\tilde{z}[k] \triangleq r_d[k] - \tilde{a}[k]$ is obtained (see Fig. 1). The prediction–error filter is designed to minimize the variance of the prediction–error $\Delta\tilde{z}[k]$ for the case $\tilde{a}[k] = a[k]$. Thus, the estimated symbol $\hat{a}[k] \in \mathcal{A}$ is that one which minimizes $|\Delta\tilde{z}[k]|^2$. As indicated in Fig. 1, the resulting noise prediction–error filter needs knowledge of the current trial symbol $\tilde{a}[k]$, previously decided symbols $\hat{a}[k-\nu]$, $\nu \geq 1$, and $\hat{z}[k-\nu] \triangleq r_d[k-\nu] - \hat{a}[k-\nu]$, $\nu \geq 1$.

3. NOISE PREDICTION USING AN FIR FILTER

In this section an FIR filter is applied for noise prediction. For derivation of the filter it is assumed that $\tilde{a}[k] = a[k]$ and $\hat{a}[k-\nu] = a[k-\nu]$, $\nu \geq 1$. Therefore, the filter input signal is

$$\begin{aligned} z[k] = r_d[k] - a[k] = b[k]n^*[k-1] + b^*[k-1]n[k] \\ + n[k]n^*[k-1]. \end{aligned} \tag{6}$$

It can be shown by straightforward calculations that the effective noise $z[k]$ has the covariance sequence $\mathcal{E}\{z[k+\lambda]z^*[k]\} = \sigma_z^2\delta[\lambda]$, where σ_z^2 denotes the variance of $z[k]$ and $\delta[\lambda]$ is the unit pulse sequence, i.e., $\delta[0] = 1$, $\delta[\lambda] = 0$, $\lambda \neq 0$. In spite of this fact, $z[k]$ is not a *proper* discrete complex random process [10] because the pseudo–covariance sequence $\mathcal{E}\{z[k+\lambda]z[k]\}$ does not vanish identically. By exploiting $z[\cdot]$ together with $z^*[\cdot]$ this can be used for noise prediction in order to lower the effective noise variance. Hence, the proposed prediction filter uses the samples $z^*[k-1]$, $z^*[k-2]$, $\ldots$, $z^*[k-N]$ for estimation of $z[k]$, too. The prediction–error $\Delta z[k]$ may be expressed as

$$\begin{aligned} \Delta z[k] &= z[k] - \sum_{\nu=1}^{N} \alpha_\nu[k] z[k-\nu] - \sum_{\nu=1}^{N} \beta_\nu[k] z^*[k-\nu] \\ &= -\sum_{\nu=0}^{N} \alpha_\nu[k] z[k-\nu] - \sum_{\nu=0}^{N} \beta_\nu[k] z^*[k-\nu], \end{aligned} \tag{7}$$

where $\alpha_\nu[k]$ and $\beta_\nu[k]$, $1 \leq \nu \leq N$, are the complex–valued predictor coefficients to be determined and $\alpha_0[k] \triangleq -1$, $\beta_0[k] \triangleq 0$, $\forall k$, are defined for convenience. Dependence of the coefficients on time k has been introduced because later it will turn out that the optimum coefficients indeed are time–variant. In this context it is important to note that complex conjugation is not a linear operation, i.e., it is impossible to obtain $z^*[\cdot]$ from $z[\cdot]$ by linear filtering. Therefore the introduction of the complex conjugated process $z^*[\cdot]$ in Eq. (7) is unavoidable. Using the fact that $n[k]$ is an equivalent baseband uncorrelated Gaussian noise process, i.e.,

$$\mathcal{E}\{n[k+\lambda]n^*[k]\} = \sigma^2\delta[\lambda] \tag{8}$$

and

$$\mathcal{E}\{n[k+\lambda]n[k]\} = 0, \quad \forall\ \lambda, \tag{9}$$

the variance $\sigma_{\Delta z}^2$ of the prediction–error $\Delta z[k]$ can be calculated from Eqs. (6), (7), (8) and (9):

$$\begin{aligned} \sigma_{\Delta z}^2 = \mathcal{E}\{|\Delta z[k]|^2\} = \sigma^2 \Bigg(1 + \sum_{\nu=0}^{N} \Big(& |\alpha_\nu[k]b[k-\nu] \\ & + \beta_{\nu+1}[k]b[k-2-\nu]|^2 + |\alpha_{\nu+1}[k]b^*[k-2-\nu] \\ & + \beta_\nu[k]b^*[k-\nu]|^2 \Big) \Bigg) \\ & + \sigma^4 \left(\sum_{\nu=0}^{N} |\alpha_\nu[k]|^2 + \sum_{\nu=0}^{N} |\beta_\nu[k]|^2 \right), \end{aligned} \tag{10}$$

where the definitions $\alpha_{N+1}[k] \triangleq 0$, $\beta_{N+1}[k] \triangleq 0$, $\forall k$, are used and knowledge of $b[k-\nu]$, $0 \le \nu \le N+1$, is assumed, i.e., expectation is performed only over the noise process $n[\cdot]$. The optimum predictor coefficients are chosen to minimize $\sigma^2_{\Delta z}$. Thus, Eq. (10) is differentiated with respect to $\alpha^*_\nu[k]$ and $\beta^*_\nu[k]$, $1 \le \nu \le N$, using the method for complex differentiation described in [11], Appendix B:

$$\begin{aligned}\frac{\partial \sigma^2_{\Delta z}}{\partial \alpha^*_\nu[k]} = \sigma^2 \big(&(\alpha_\nu[k] b[k-\nu] \\ &+\beta_{\nu+1}[k] b[k-2-\nu]) b^*[k-\nu] \\ &+(\alpha_\nu[k] b^*[k-1-\nu] \\ &+\beta_{\nu-1}[k] b^*[k+1-\nu]) b[k-1-\nu] \big) + \sigma^4 \alpha_\nu[k], \end{aligned} \tag{11}$$

$$\begin{aligned}\frac{\partial \sigma^2_{\Delta z}}{\partial \beta^*_\nu[k]} = \sigma^2 \big(&(\alpha_{\nu-1}[k] b[k+1-\nu] \\ &+\beta_\nu[k] b[k-1-\nu]) b^*[k-1-\nu] \\ &+(\alpha_{\nu+1}[k] b^*[k-2-\nu] \\ &+\beta_\nu[k] b^*[k-\nu]) b[k-\nu] \big) + \sigma^4 \beta_\nu[k]. \end{aligned} \tag{12}$$

By setting Eqs. (11) and (12) equal to zero and applying Eq. (1), $2N$ equations for determination of $2N$ coefficients are obtained ($1 \le \nu \le N$):

$$\begin{aligned}(2+\sigma^2)\alpha_\nu[k] + \beta_{\nu-1}[k] u^*[k+1-\nu] \\ +\beta_{\nu+1}[k] u^*[k-\nu] = 0, \end{aligned} \tag{13}$$

$$\begin{aligned}(2+\sigma^2)\beta_\nu[k] + \alpha_{\nu-1}[k] u[k+1-\nu] \\ +\alpha_{\nu+1}[k] u[k-\nu] = 0, \end{aligned} \tag{14}$$

where the notation $u[k] \triangleq a[k]a[k-1]$ has been used. From Eqs. (13) and (14) it follows that N coefficients are always zero:

$$\alpha_1[k] = \beta_2[k] = \alpha_3[k] = \beta_4[k] = \ldots = \xi_N[k] = 0, \tag{15}$$

where $\xi_N[k]$ is $\alpha_N[k]$ ($\beta_N[k]$) if N is odd (even). The remaining N coefficients can be calculated from

$$\mathbf{A}\mathbf{x} = \mathbf{y}, \tag{16}$$

where the $N \times N$ matrix $\mathbf{A}$ and the $N \times 1$ vectors $\mathbf{x}$ and $\mathbf{y}$ are defined as

$$\mathbf{A} = \begin{pmatrix} 2+\sigma^2 & u[k-1] & 0 & \ldots & \ldots & 0 \\ u^*[k-1] & 2+\sigma^2 & u^*[k-2] & 0 & \ldots & 0 \\ 0 & u[k-2] & 2+\sigma^2 & u[k-3] & \ddots & \ddots \\ \vdots & \ddots & \ddots & \ddots & \ddots & \ddots \end{pmatrix}, \tag{17}$$

$$\mathbf{y} = (u[k]\ 0\ \ldots\ 0)^T, \tag{18}$$

$$\mathbf{x} = (\beta_1[k]\ \alpha_2[k]\ \beta_3[k]\ \alpha_4[k]\ \ldots)^T. \tag{19}$$

Here, $(\cdot)^T$ denotes the transpose of a vector and the last (Nth) element of $\mathbf{x}$ is $\alpha_N[k]$ ($\beta_N[k]$) if N is even (odd).

In contrast to usual predictors, this prediction filter is time–variant because its coefficients depend on former data symbols and the current data symbol to be estimated. In a most simple structure decision feedback is applied. Thus, in Eq. (7) $\hat{a}[k-\nu]$ is used instead of $a[k-\nu]$, $1 \le \nu \le N$, for calculation of the filter coefficients and the state variables, i.e., $\hat{z}[k-\nu] = r_d[k-\nu] - \hat{a}[k-\nu]$, $1 \le \nu \le N$, are used instead of $z[k-\nu]$, whereas the current symbol decision $\hat{a}[k]$ is chosen in that way that $|\Delta\tilde{z}[k]|^2$ is minimized (see Fig. 1). Notice, that in Eq. (7) $z[k]$ has to be replaced by $\tilde{z}[k] = r_d[k] - \tilde{a}[k]$, too.

In contrast to classical decision–feedback noise prediction, M different prediction errors $\Delta\tilde{z}[k]$ have to be calculated. But this corresponds to an only moderate increase in complexity. In more complex receiver structures all combinations for $L \le N$ past trial symbols $(\tilde{a}[k-1], \tilde{a}[k-2], \ldots, \tilde{a}[k-L])$ may be taken into consideration, whereas residual past symbols are taken from decisions. Such receiver structures correspond to reduced–state sequence estimation and a continuous tradeoff between performance and complexity is possible via variation of L.

Examples

1. $N = 1$: In this case, Eqs. (15) and (16) yield

$$\alpha_1[k] = 0, \tag{20}$$

$$\beta_1[k] = \frac{a[k]a[k-1]}{2+\sigma^2}. \tag{21}$$

$\beta_1[k]$ depends on the variance σ^2. However, simulations show that for the practical interesting case $10\log_{10}(E_b/N_0) > 4$ dB this dependence is negligible. Thus, $\beta_1[k] = \frac{1}{2}a[k]a[k-1]$ can be used instead of Eq. (21). Because $a[k]$ and $a[k-1]$ are unknown at the receiver, $\tilde{a}[k]$ and the feedback symbol $\hat{a}[k-1]$ are used. Thus, Eq. (21) is replaced by

$$\beta_1[k] = \frac{1}{2}\tilde{a}[k]\hat{a}[k-1]. \tag{22}$$

Fig. 2a) shows the prediction–error filter for $N = 1$.

2. $N = 2$: Now the filter coefficients calculated from Eqs. (15) and (16) are

$$\alpha_1[k] = 0, \tag{23}$$

$$\beta_1[k] = \frac{2+\sigma^2}{3+4\sigma^2+\sigma^4}\, a[k]a[k-1], \tag{24}$$

$$\alpha_2[k] = -\frac{1}{3+4\sigma^2+\sigma^4}\, a[k]a^*[k-2], \tag{25}$$

$$\beta_2[k] = 0. \tag{26}$$

Like in the case $N = 1$, the dependence of $\beta_1[k]$ and $\alpha_2[k]$ on σ^2 was neglected in the simulations

shown in Section 5. Using again $\tilde{a}[k]$ and previously decided symbols, the following filter coefficients result:

$$\beta_1[k] = \frac{2}{3}\tilde{a}[k]\hat{a}[k-1], \tag{27}$$

$$\alpha_2[k] = -\frac{1}{3}\tilde{a}[k]\hat{a}^*[k-2]. \tag{28}$$

The prediction–error filter for $N = 2$ is shown in Fig. 2b).

For $N > 2$ the filter coefficients can be obtained again from Eqs. (15) and (16). As N increases, the detector performance improves, however, the detector becomes more complex. Therefore, it is desirable to change the structure of the noise prediction–error filter to get good performance at low computational complexity. Such a modified structure is presented in the next section.

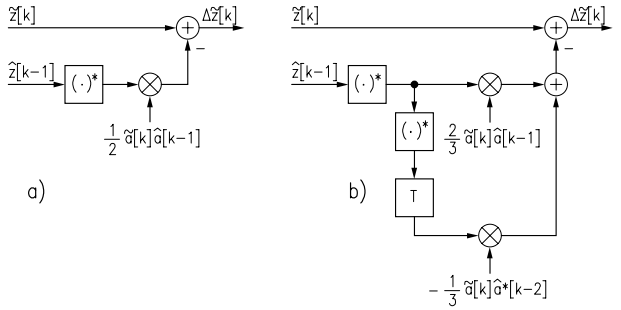

Figure 2: Noise prediction using an FIR filter: a) $N = 1$; b) $N = 2$.

4. NOISE PREDICTION USING AN IIR FILTER

For reasonable high SNRs, the term $n[k]n^*[k-1]$ in Eq. (6) becomes negligible and $z[k]$ consists essentially of a weighted sum of $n[k]$ and $n^*[k-1]$, which corresponds to a nonlinear time–variant FIR filter structure. Therefore, a prediction–error filter which reduces the variance of $z[k]$ most efficiently has a first order nonlinear time–variant IIR structure. The structure of the IIR prediction–error filter, if perfect knowlege of $a[k-\nu]$, $\nu \geq 0$, is assumed, is shown in Fig. 3a). Since $z[k]$ contains the term $n[k]n^*[k-1]$, too, it is necessary to optimize the time–variant coefficient $\gamma[k]$ in order to get the lowest possible variance of $\Delta z[k]$. As can be seen from Fig. 3a), the prediction–error is

$$\Delta z[k] = z[k] - \gamma[k]\Delta z^*[k-1]. \tag{29}$$

To simplify the analysis it is assumed that the number of symbols already transmitted is infinite. Taking this into account and using the recursive structure of Eq. (29),

$$\begin{aligned}\Delta z[k] = z[k] &- \gamma[k]z^*[k-1] + \gamma[k]\gamma^*[k-1]z[k-2] \\ &-\gamma[k]\gamma^*[k-1]\gamma[k-2]z^*[k-3] + \ldots\end{aligned} \tag{30}$$

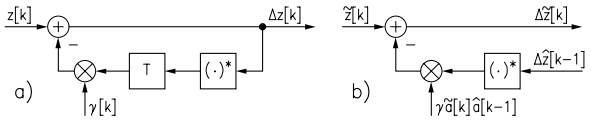

Figure 3: a) IIR noise prediction–error filter if perfect knowlege of $a[k-\nu]$, $\nu \geq 0$, is assumed; b) implementable structure corresponding to Fig. 3a)

is obtained. Using Eqs. (1), (6), (8), (9), (30), and again the notation $u[k] = a[k]a[k-1]$, $\sigma^2_{\Delta z}$ can be calculated according to

$$\begin{aligned}\sigma^2_{\Delta z} = \mathcal{E}\{|\Delta z[k]|^2\} &= \sigma^2\big(1 + |u[k] - \gamma[k]|^2 \\ &+|\gamma[k]|^2|u[k-1] - \gamma[k-1]|^2 \\ &+|\gamma[k]|^2|\gamma[k-1]|^2|u[k-2] - \gamma[k-2]|^2 + \ldots\big) \\ &+\sigma^4\big(1 + |\gamma[k]|^2 + |\gamma[k]|^2|\gamma[k-1]|^2 + \ldots\big).\end{aligned} \tag{31}$$

By choosing the filter coefficient $\gamma[k]$ properly, $\sigma^2_{\Delta z}$ can be made smaller than the variance of $z[k]$. Eq. (31) suggests the empirical choice

$$\gamma[k] = \gamma u[k] = \gamma a[k]a[k-1], \tag{32}$$

where γ is a real number satisfying $0 \leq \gamma < 1$. Since $a[k]$ and $a[k-1]$ are unknown, the trial symbol $\tilde{a}[k]$ and the decision feedback symbol $\hat{a}[k-1]$ are used in an implementation. Therefore, $\Delta z[k]$ in Eq. (29) is replaced by $\Delta\tilde{z}[k]$, which is calculated for all M possible values of the trial symbol $\tilde{a}[k]$. Moreover, $\Delta\hat{z}[k-1]$ is used instead of $\Delta z[k-1]$ in Eq. (29). Note, that $\Delta\hat{z}[k-1]$ is that $\Delta\tilde{z}[k-1]$ out of M with minimum $|\Delta\tilde{z}[k-1]|^2$. Fig. 3b) shows the corresponding structure.

Inserting Eq. (32) into Eq. (31) yields

$$\begin{aligned}\sigma^2_{\Delta z} &= \sigma^2\left(1 + (1-\gamma)^2\sum_{\nu=0}^{\infty}\gamma^{2\nu}\right) + \sigma^4\sum_{\nu=0}^{\infty}\gamma^{2\nu} \\ &= \frac{2\sigma^2}{1+\gamma} + \frac{\sigma^4}{1-\gamma^2}.\end{aligned} \tag{33}$$

Fig. 4a) illustrates Eq. (33) for a QDPSK ($M = 4$, $\sigma^2 = \frac{N_0}{2E_b}$, where E_b is the (mean) received energy per bit) constellation. Notice, that the curve for $\gamma = 0$ corresponds to a conventional differential detector. Obviously, the variance of $\Delta z[k]$ can be reduced by increasing γ. However, at low E_b/N_0 ratios $\sigma^2_{\Delta z}$ increases if γ is choosen too large. This suggests that an optimum γ exists for each σ^2 (E_b/N_0), which can be calculated by differentiating Eq. (33) with respect to γ and setting the result equal to zero. If the constraint $0 \leq \gamma < 1$ is taken into account,

$$\gamma_{\text{opt}} = 1 + \frac{\sigma^2}{2} - \sigma\sqrt{1 + \frac{\sigma^2}{4}} \tag{34}$$

is obtained. Fig. 4b) illustrates the dependence of γ_{opt} on E_b/N_0 for QDPSK. By inserting γ_{opt} from Eq. (34)

into Eq. (33) the minimum variance of the prediction–error can be calculated to

$$\sigma^2_{\Delta z} = \sigma^2 \frac{1}{1 + \frac{\sigma^2}{2} - \sigma\sqrt{1 + \frac{\sigma^2}{4}}} = \frac{\sigma^2}{\gamma_{\text{opt}}}. \qquad (35)$$

From Eq. (35) it follows that the variance of $\Delta z[k]$ tends to σ^2 for $\sigma^2 \ll 1$. According to Eq. (34), the corresponding γ_{opt} tends to 1. In this case, $\Delta z[k] \to b^*[k-1]n[k]$, cf. Eqs. (30), (6), (32), which implies, that a Gaussian random variable results asymptotically. This means that the proposed detector has the same performance as a coherent detector in the high SNR region, since in both cases the decision variable has a Gaussian probability density function with variance σ^2.

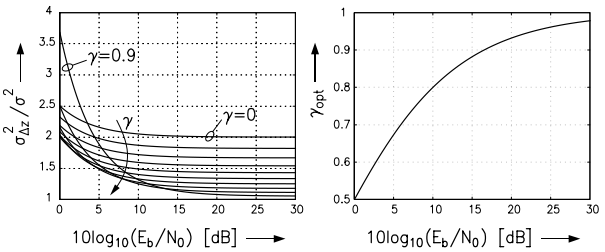

Figure 4: a) Normalized variance $\frac{\sigma^2_{\Delta z}}{\sigma^2}$ vs. E_b/N_0 for QDPSK; γ varies from 0 to 0.9 in steps of 0.1; b) optimum filter coefficient γ_{opt} vs. E_b/N_0 for QDPSK.

Equivalent low–complexity decision rule

Using the decision rule described above, it is necessary to calculate all M possible values of $|\Delta\tilde{z}[k]|^2$ in order to determine $\hat{a}[k]$. However, an equivalent low–complexity decision rule can be derived. According to Fig. 3b), $|\Delta\tilde{z}[k]|^2$ may be written as

$$|\Delta\tilde{z}[k]|^2 = |r_d[k]|^2 + |\tilde{a}[k]|^2\,|1 + \gamma\hat{a}[k-1]\Delta\hat{z}^*[k-1]|^2 - 2\text{Re}\left\{\tilde{a}^*[k](1 + \gamma\hat{a}[k-1]\Delta\hat{z}^*[k-1])^* r_d[k]\right\}, \qquad (36)$$

where $\tilde{z}[k] = r_d[k] - \tilde{a}[k]$ has been used. Since the first two terms in Eq. (36) are common to all possible $\tilde{a}[k]$, they can be omitted. The minimum is attained when the real part of $\tilde{a}^*[k](1 + \gamma\hat{a}[k-1]\Delta\hat{z}^*[k-1])^* r_d[k]$ becomes maximum, i.e., the phase of $\tilde{a}[k]$ is next to the phase of $(1 + \gamma\hat{a}[k-1]\Delta\hat{z}^*[k-1])^* r_d[k]$. This means, that like for a conventional differential detector the complex plain can be divided into M sectors and $\hat{a}[k]$ is determined by the sector into which the complex number $(1 + \gamma\hat{a}[k-1]\Delta\hat{z}^*[k-1])^* r_d[k]$ falls. Note, that for $\gamma = 0$ this corresponds to DD. Starting from Figs. 2a) and 2b), it is possible to derive a similar low complexity decision rule for both FIR filter orders discussed.

5. SIMULATION RESULTS

In Fig. 5 the performance of the proposed receiver structures is compared with conventional DD and CD for QDPSK ($M = 4$) and AWGN conditions. It can be seen that noise prediction using an FIR filter can improve the power efficiency of a differential detector significantly even at low predictor orders. For example, at a BER of 10^{-3} and for $N = 1$ there is an improvement of about 0.6 dB in E_b/N_0 compared to DD, whereas the improvement is about 1 dB for $N = 2$. As the order of the noise prediction filter increases, performance improves, but of course is always inferior to that of CD. Fig. 5 contains also two curves for noise prediction using an IIR filter. As already expected from Fig. 4a), $\gamma = 0.7$ yields a better result than $\gamma = 0.3$ because of the lower noise variance for $10\log_{10}(E_b/N_0) > 1$ dB. At BER $= 10^{-3}$ the IIR noise predictor improves the performance of DD by about 1.2 dB and the difference between CD and the proposed scheme is only about 0.6 dB. As can be concluded from Fig. 4a), a further increase of γ would improve the detector performance at high E_b/N_0 ratios. In the limit ($\gamma \to 1$, $\sigma^2 \to 0$) the new technique approaches CD, as already stated in the previous section. However, at low E_b/N_0 ratios, the performance of the IIR noise prediction detector deteriorates, since there, the variance of $\Delta z[k]$ increases if γ is chosen too large.

In practice, it is desirable to have a fixed value for γ. Here $\gamma = 0.7$ would be a good choice because, as can be seen from Fig. 4a), for $\gamma > 0.7$ the noise variance reduction at high E_b/N_0 ratios is small, whereas the degradation at low E_b/N_0 ratios is significant. Therefore $\gamma = 0.7$ is used for a comparison with the noncoherent detection scheme proposed in [4, 5] for AWGN, flat Rayleigh and Ricean fading channels. In all fading simulations Jakes model [12] was used. The normalized Doppler frequency f_dT has been chosen to 0.0075 (corresponding to worst case in IS–136 digital cellular standard) and 0.03 (corresponding to worst case in [5]) for Rayleigh and Ricean fading, respectively. The Ricean factor R [9] for the Ricean fading channel was 7 dB. The IIR filter coefficient α defined in [5] was chosen to 0.6 in order to get approximately the same performance as for $\gamma = 0.7$ for AWGN conditions. Fig. 6 shows that in this case both techniques perform better than DD. In many applications (for example terrestrial and satellite mobile communications) the receiver has to cope with both, AWGN and flat fading channels. As can be seen from Fig. 6, for fading conditions the IIR noise prediction detector has the same power efficiency as DD[1] and outperforms the detection scheme proposed in [4, 5] which causes an error floor

[1]The BERs for DD shown in Fig. 8 of [5] for Ricean fading ($f_dT = 0.03$, $R = 7$ dB) are slightly higher than in Fig. 6 of this paper. Presumably this is due to the fast acquisition clock recovery used there, whereas perfect synchronisation is assumed here.

nearly twice as high. Note, that the filter coefficients of both schemes were constant for all channel models. It should be mentioned, that $\alpha > 0.6$ would improve performance for the AWGN channel, but would cause a significant degradation for fading channels. In general, a Ricean factor estimation circuit proposed in [5] would reduce the error floor for the technique there, however, computational complexity would increase considerably.

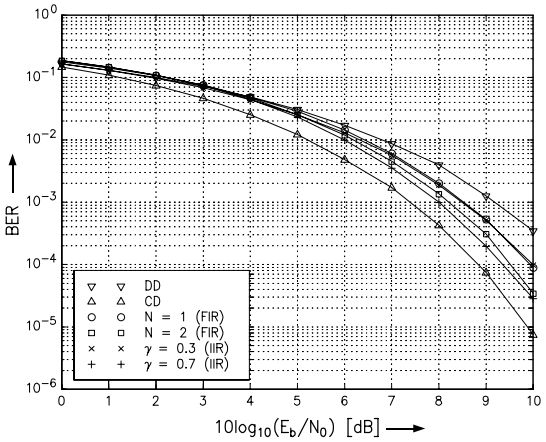

Figure 5: BER of QDPSK ($M = 4$) vs. E_b/N_0 for DD, CD, and noise prediction with FIR and IIR filter under AWGN conditions.

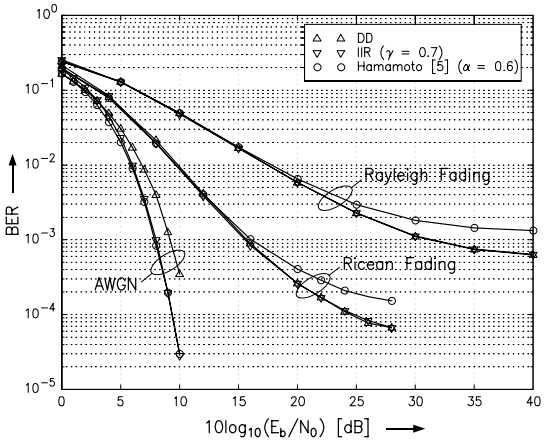

Figure 6: BER of QDPSK ($M = 4$) vs. E_b/N_0 for DD, noise prediction with IIR filter, and the scheme proposed in [4, 5] for AWGN, Rayleigh fading ($f_dT = 0.0075$), and Ricean fading ($R = 7$ dB, $f_dT = 0.03$) channels.

6. CONCLUSIONS

In this paper, a new technique has been proposed in order to improve the performance of DD for AWGN channels. The noise in the decision variable is reduced by means of noise prediction. Optimum coefficients for FIR and IIR prediction–error filters have been calculated. Simulations show for both cases that the power efficiency of a conventional differential detector is improved considerably. For the IIR structure a simplified decision rule has been derived which makes this structure particularly interesting for implementation because of its very low computational complexity. It turns out that the proposed detector yields a good overall performance when the IIR filter coefficient γ is chosen around 0.7. In this case, DD is improved by 1.2 dB at a BER of 10^{-3} for AWGN conditions while no performance degradation compared to DD is observed for Rayleigh and Ricean fading channels. In contrast to that, the low complexity detector presented in [4, 5] degrades considerably under fading conditions as has been demonstrated by simulations.

ACKNOWLEDEGMENT

The authors would like to thank TCMC (Technology Centre for Mobile Communication), Philips Semiconductors, Germany, for supporting this work.

REFERENCES

[1] D. Divsalar, M. K. Simon: Multiple-Symbol Differential Detection of MPSK, *IEEE Trans. Commun.*, Vol. 38, 1990, pp. 300 - 308.

[2] K. M. Mackethun, Jr.: A Fast Algorithm for Multiple-Symbol Differential Detection of MPSK, *IEEE Trans. Commun.*, Vol. 42, 1994, pp. 1471 - 1474.

[3] F. Edbauer: Bit Error Rate of Binary and Quaternary DPSK Signals with Multiple Differential Feedback Detection, *IEEE Trans. Commun.*, Vol. 40, 1992, pp. 457 -460.

[4] H. Leib: Data–Aided Noncoherent Demodulation of DPSK, *IEEE Trans. Commun.*, Vol. 43, 1995, pp. 722 - 725.

[5] N. Hamamoto: Differential Detection with IIR Filter for Improving DPSK Detection Performance, *IEEE Trans. Commun.*, Vol. 44, 1996, pp. 959 - 966.

[6] H. Leib: Comments on "Differential Detection with IIR Filter for Improving DPSK Detection Performance", *IEEE Trans. Commun.*, Vol. 45, 1997, p. 637.

[7] F. Adachi, M. Sawahashi: Decision Feedback Differential Phase Detection of M-ary DPSK Signals, *IEEE Trans. Vehic. Technol.*, Vol. 44, 1995, pp. 203 - 210.

[8] R. Y. Wei, M. C. Lin: Differential Phase Detection Using Recursively Generated Phase References, *IEEE Trans. Commun.*, Vol. 45, 1997, pp. 1504 - 1507.

[9] T. S. Rappaport: *Wireless Communications*, Prentice Hall, New Jersey, 1996.

[10] F. D. Neeser, J. L. Massey: Proper Complex Random Processes with Applications to Information Theory, *IEEE Trans. Infor. Theory*, Vol. 39, 1993, pp. 1293 - 1302.

[11] S. Haykin: *Adaptive Filter Theory*, 3rd edition, Prentice Hall, New Jersey, 1996.

[12] W. C. Jakes, Jr., Ed., *Microwave Mobile Communications*, Wiley, New York, 1974.